Critical behavior of the two-dimensional XY model: A Monte Carlo simulation

Julio F. Fernández*
Centro de Física, Instituto Venezolano de Investigaciones Científicas, Apartado 1827, Caracas 1010A, Venezuela

Manuel F. Ferreira†
Departamento de Física, Universidad Simón Bolívar, Apartado 80659, Caracas 1080A, Venezuela

Jolanta Stankiewicz‡
IBM Thomas J. Watson Research Center, Yorktown Heights, New York 10598
(Received 29 January 1986)

We have performed Monte Carlo (MC) simulations on systems of $L\times L$ classical planar unit spins on square lattices, for $L=6$, 15, 30, 60, 90, and 200. The interaction between any two given spins $\vec{S}_1$ and $\vec{S}_2$ is given by $-J\vec{S}_1\cdot\vec{S}_2$ if S_1 and S_2 are nearest neighbors and vanishes otherwise. In order to make sure that our results correspond to equilibrium values, we have looked into the time-dependent properties of this model in the vicinity of critical temperature (T_c). We have found that the diffusion constant for vortex motion is given at T_c by $D\simeq 0.2$ (in units of nearest-neighbor distance squared per MC step per spin). The values of the relaxation times follow from the value of D. Our computer running times were typically 10^5 MC steps per spin, larger than any relaxation time for the system sizes we deal with. We use a procedure based on finite-size scaling to establish the value of $T_c=0.89J/k_B$, the value of $\nu=0.5\pm 0.1$, and the value of $\eta_c=0.24\pm 0.03$, in agreement with the values predicted by the Kosterlitz-Thouless theory.

I. INTRODUCTION

Kosterlitz and Thouless[1] (KT) developed some years ago the currently accepted theory of the critical behavior of the XY model in two dimensions (2D). Additional theoretical work published since then supports this theory.[2,3] However there are very few experimental or computational verifications of the value of ν, the index governing the critical divergence of the correlation length (ξ). Monte Carlo (MC) simulations[4] have produced values close to $\nu=0.7$, but with errors that are overly large. Other calculations often[5] give results somewhat different from the value $\nu=0.5$ predicted by KT.

Experimental work has been reported on the critical behavior of He^4 films,[6] superconducting films[7] and two dimensional arrays of superconducting grains[8] all closely related to the XY model in 2D.[9] The critical value, $\eta(T_c)=\frac{1}{4}$, predicted by KT (η is defined by $\langle S_0 S_r\rangle \sim r^{-\eta}$ below T_c) has been approximately confirmed. The value of ν predicted by KT also fits experimental results well but with errors in the value of ν about 0.1, originated in uncertainties in the value of T_c.[7]

We have performed fairly long MC calculations (typically, 10^5 MC steps per spin) on systems of $L\times L$ spins for $L=6$, 15, 30, 60, 90, and 200. We are interested in the quantity,

$$\mathcal{S}=L^{-2}\sum\langle \mathbf{S}_j\cdot\mathbf{S}_j\rangle\ , \tag{1.1}$$

where $\mathbf{S}_i$ is a classical unit spin at the ith site and the sum is over all i and j sites. We use the relation

$$\mathcal{S}\sim L^{2-\eta}\ , \tag{1.2}$$

valid for $T\le T_c$, to obtain $\eta(T)$ from plots of $\ln(\mathcal{S})$ versus $\ln(L)$. We have determined: (a) the value $\eta(T_c)=0.24\pm 0.03$ in agreement with $\eta(T_c)=\frac{1}{4}$, predicted by Kosterlitz and Thouless, and (b) the value of $T_c=(0.89\pm 0.02)\ J/k_B$, in close agreement with the value of T_c obtained previously[4,10] in MC simulations.

Kosterlitz and Thouless derived for the correlation length (ξ) the expression

$$\xi(T)=\xi_0\exp[b/(T-T_c)^{\nu}]\ , \tag{1.3}$$

where ξ_0 and b are nonuniversal constants and ν is the critical index which interests us here. To determine ν, we use a procedure based on the finite-size scaling[11,12] relation

$$\mathcal{S}\sim L^{2-\eta}F(\tilde{\xi}/L)\ , \tag{1.4}$$

where $\tilde{\xi}=\xi/\xi_0$, which serves to define the scaling function F.

We are able to establish the result

$$\nu=0.5\pm 0.1\ . \tag{1.5}$$

The method we use to arrive at this result accounts for finite-size effects and should be quite useful to analyze critical behavior data obtained in experiments on granular superconductors.

We have taken care to make our computer running times sufficiently long to be able to obtain equilbrium results. We have computed equilibrium relaxation times (τ) for the time dependent correlation $\langle \mathbf{M}\cdot\mathbf{M}(t)\rangle$, where $\mathbf{M}$ is the total magnetization of the system. We have also computed the diffusion constant (D) for vortex motion for

$T \simeq T_c$. D and τ are related, for the time (τ_v) it takes one vortex to diffuse across the length (L) of the system is given by

$$L^2 = D\tau_v \ , \tag{1.6}$$

and since there is one vortex in the system at $T=T_c$,[13] it follows that τ_v is about the same as the time it takes $\mathbf{M}$ to relax. Incidently, we have obtained $D \simeq 0.2$ at $T=T_c$. We have also checked that our results are independent of the initial state.

The plan of the paper is as follows. In Sec. II we first compute relaxation times for $\mathbf{M}$ and the diffusion constant for vortices near T_c. In order to obtain equilibrium results our running times are longer than the corresponding values of τ. We then describe how we determine $\eta(T)$ from our MC generated data. We next describe three different procedures we follow to determine the value $\nu = 0.5$. Two of these procedures are based on finite-size scaling. Only one of them yields an error in ν which is (0.1) not overly large. In Sec. III we discuss our results and argue that $\eta_c = 0.24 \pm 0.03$. All values of the temperature are given in units of J/k_B.

II. RESULTS

We have used the standard Metropolis Monte Carlo algorithm[14] on systems of $L \times L$ classical planar spins on square lattices $L = 6$, 15, 30, 60, 90, and 200. Usually, the first MC run for each system was performed at some high temperature well above T_c. The directions of all spins were initially random for the first run. The state obtained at the end of each run was used as the initial state of the following run at the next lower temperature. For each run, we first allowed the system to equilibrate for a time (in units of MC steps per spin) comparable to the relaxation time (see Sec. II A below for its definition and calculation) followed by a longer time during which equilibrium quantities were computed. Typically, 10^5 MC steps per spin were taken for $T < 1$, which is about $1.1\,T_c$. For $T \geq 1$ our runs were shorter, but none under 4×10^4 MC steps per spin.

In the following subsection we examine the relaxation behavior of the system in order to show that our runs are sufficiently long to yield equilibrium values.[15]

A. Relaxation times

A relaxation time (τ) can be defined through the correlation function,

$$\mathcal{S}(t) = \langle \mathbf{M} \cdot \mathbf{M}(t) \rangle \ , \tag{2.1}$$

which we obtain using

$$\langle \mathbf{M} \cdot \mathbf{M}(t) \rangle = \frac{1}{m} \sum_{n=1}^{m} \mathbf{M}(t_n) \mathbf{M}(t_n + t) \ , \tag{2.2}$$

where $\mathbf{M} = (\sum S_i^x, \sum S_i^y)$ and t_n stands for the time corresponding to the nth MC step per spin *after* equilibrium has been achieved. We define,[16]

$$\tau = \int_0^\infty \mathcal{S}(t) dt / \mathcal{S}(0) \ . \tag{2.3}$$

At $T = 0.89$ (i.e., $T \simeq T_c$), the values we have obtained obey the relation

$$\tau \approx 2L^2 \ , \tag{2.4}$$

which for our most severe case ($L = 200$) yields $\tau \approx 8 \times 10^4$ MC steps per spin.

This equation is expected on the basis of the following simple picture:[17] at T_c, there is typically only one vortex present[13] in the system and it diffuses across the system in the time τ_v given by

$$L^2 = D\tau_v \ , \tag{2.5}$$

where D is a diffusion constant. As the vortex diffuses, $\mathbf{M}$ rotates and consequently $\tau_v \sim \tau$. This argument supports Eq. (2.4) and leads one to expect $D \sim 0.5$ at T_c.

We have checked the argument above by computing D directly at T_c,

$$D(T_c) \simeq 0.2 \ , \tag{2.6}$$

in units of (nearest-neighbor distance)^2/MC step per spin.[18] Thus, disregarding factors of 2 or 3, we see that vortex motion does indeed account for the time relaxation of $\mathbf{M}$ and gives us confidence in the validity of Eqs. (2.1) and (2.3).

To compute the value of D, we set up a vortex at some point in the system ($x=0$, $y=0$, by definition) at some time ($t=0$) after the system has reached equilibrium. Let the position of the vortex, n MC steps after $t=0$ be $\mathbf{r}(t_n)$, then

$$D = \frac{1}{m} \sum_{n=1}^{m} [\mathbf{r}(t_n)]^2 / t_n \tag{2.7}$$

in the $m \to \infty$ limit yields the correct value of D for an infinite size system. We have arrived at the value of D quoted for T_c using the above expression for $m \sim 10^3$ and $L = 15$, 30, and 60.

Finally, many runs were repeated starting from different initial states: either all spins parallel, or all spins

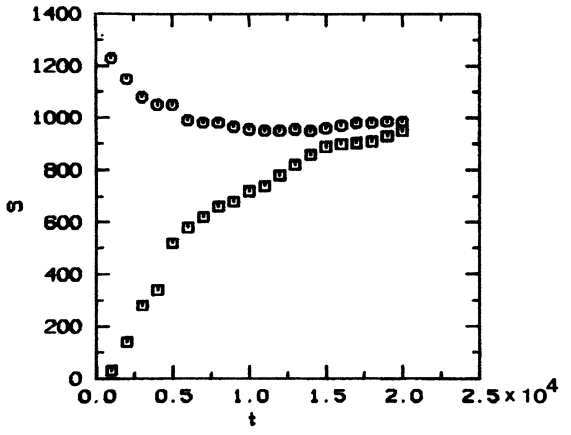

FIG. 1. Quantity $\mathcal{S}$, defined in Eq. (1.1) is shown for a system of 60×60 spins, at $T = 0.92$, versus the time (in units of MC steps per spin) over which the average indicated in Eq. (1.1) has been taken, starting from two different initial conditions: (i) all spins parallel (⊙), and (ii) all spins initially at random (⊡). Note that, as expected, both curves approach each other for $t \gtrsim \tau$; $\tau = 7 \times 10^3$ in this case ($L = 60$), according to Eq. (2.4).

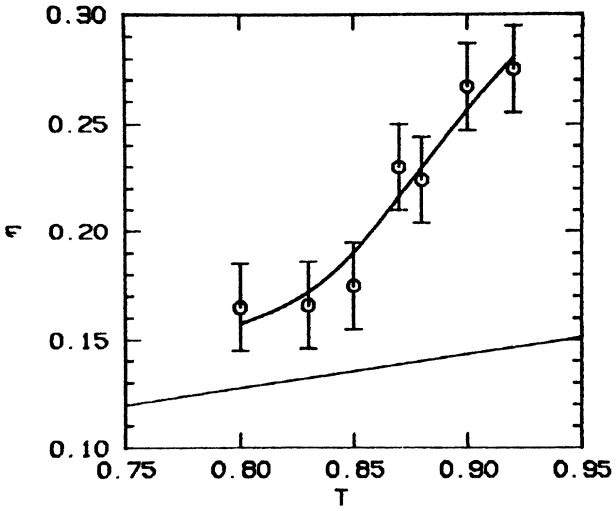

FIG. 2. Values of $\eta(T)$ obtained from curves of $\ln(\mathcal{S})$ versus $\ln(L)$ are shown. The straight line represents the spin-wave contribution $(T/2\pi)$ to η.

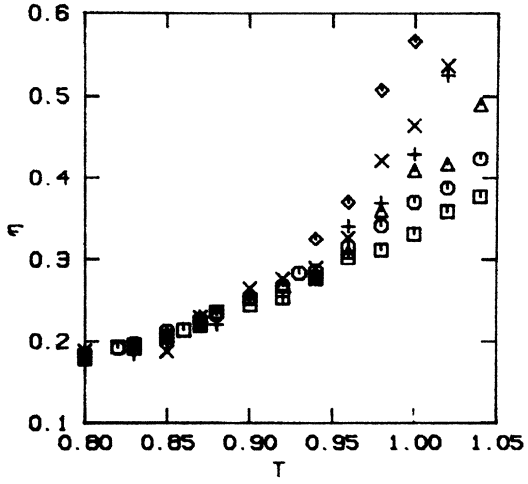

FIG. 3. $\eta(T)$ as given by Eq. (2.8) is plotted versus T for various values of L: ⊡ is for $L=6$, ⊙ is for $L=15$, Δ is for $L=30$, + is for $L=60$, × is for $L=90$, and ◈ is for $L=200$. Note that there is considerable spread of the data points for $T \gtrsim 0.9$, indicating that $T_c \approx 0.9$.

pointing in random directions. One such set of runs is shown in Fig. 1 for $l=60$ and $T=0.92$. The results obtained were, within statistical errors, independent of initial conditions for running times considerably longer than τ in every case checked. The equilibrium values obtained for $\mathcal{S}$ and the mean energy per spin (in units of J) are shown in Tables I and II, respectively.

B. Value of η

To obtain η for $T<T_c$, we compute $\mathcal{S}$, defined by Eq. (1.1). Now, since $\mathcal{S} \sim L^{2-\eta}$ for $T<T_c$, plots of $\ln\mathcal{S}$ versus $\ln L$ yield $2-\eta$ for each value of T. The values of η obtained are shown in Fig. 2. We note that the value predicted by Kosterlitz and Thouless, $\eta(T_c)=\frac{1}{4}$, occurs

TABLE I. Equilibrium values of $\mathcal{S}$, defined in Eq. (1.1), at different temperatures (in units of J/k_B) for systems of $L \times L$ spins.

	$\mathcal{S}$					
T	$L=6$	$L=15$	$L=30$	$L=60$	$L=90$	$L=200$
0.80	21.7	115	409	1490	2910	
0.83	21.2	110	386	1420	2820	
0.85	20.8	106	370	1340	2910	
0.87	20.2	102	357	1180	2410	
0.90	19.4	94.9	317	1070	2060	8560
0.92	19.1	91.1	300	1060	1950	
0.94	18.3	86.8	289	941	1840	5970
0.96	17.5	79.9	263	745	1560	4700
0.98	17.2	74.5	221	663	1020	2270
1.00	16.6	68.9	187	518	836	1660
1.02	15.8	65.8	182	350	604	708
1.04	15.3	59.7	142	246	327	387
1.06	14.6	52.5	118	197	251	220
1.08	14.2	47.5	106	165	166	169
1.10	13.5	44.6	80.8	94.4	114	95
1.12	13.9	40.7	64.5	80.1	90.0	
1.14	12.7	35.8	53.9	73.2	71.0	
1.16	12.2	32.5	47.6	54.9	62.0	
1.18	11.7	27.8	42.0	47.1	43.0	
1.20	11.0	25.2	36.0	37.4		
1.22	10.6	23.5	29.3	34.7		
1.24	10.2	20.6	25.7	26.5		
1.26	9.86	18.8	23.4	27.3		
1.28	9.31	17.25	20.4	21.4		
1.30	9.1	15.9	18.7			

TABLE II. Equilibrium values of the mean energy per spin (in units of J) at different temperatures (in units of J/k_B) for systems of $L \times L$ spins.

	Mean energy per spin					
T	$L=6$	$L=15$	$L=30$	$L=60$	$L=90$	$L=200$
0.80	−1.3572	−1.4526	−1.4883	−1.5076	−1.5141	
0.83	−1.3322	−1.4245	−1.4624	−1.4826	−1.4894	
0.85	−1.3164	−1.4076	−1.4428	−1.4658	−1.4715	
0.87	−1.2966	−1.3888	−1.4270	−1.4459	−1.453	
0.90	−1.2686	−1.3594	−1.3953	−1.4160	−1.428	−1.4315
0.92	−1.2495	−1.3375	−1.3755	−1.3975	−1.4030	
0.94	−1.2298	−1.3166	−1.3541	−1.3743	−1.3806	−1.3887
0.96	−1.2116	−1.2894	−1.3285	−1.3490	−1.3428	−1.3658
0.98	−1.1695	−1.2701	−1.3042	−1.3252	−1.3302	−1.3387
1.00	−1.1490	−1.2441	−1.2769	−1.2985	−1.3064	−1.3119
1.02	−1.127	−1.2210	−1.2546	−1.2697	−1.2785	−1.2836
1.04	−1.1076	−1.1960	−1.2250	−1.2401	−1.2472	−1.2553
1.06	−1.090	−1.1702	−1.1986	−1.2139	−1.2197	−1.2261
1.08	−1.068	−1.1406	−1.1705	−1.1914	−1.1918	−1.1978
1.10	−1.050	−1.1200	−1.1405	−1.1579	−1.1646	−1.1698
1.12	−1.029	−1.0910	−1.1153	−1.1315		
1.14	−1.008	−1.0660	−1.0903	−1.1037	−1.1076	
1.16	−0.9874	−1.0450	−1.0675	−1.0780	−1.0859	
1.18	−0.9684	−1.0090	−1.0432	−1.0552	−1.0611	
1.20	−0.9510	−0.9937	−1.0151	−1.0338		
1.22	−0.9289	−0.9703	−0.9936	−1.0109		
1.24	−0.9122	−0.9502	−0.9725	−0.9890		
1.26	−0.8958	−0.9303	−0.9523	−0.9675		
1.28	−0.8760	−0.9134	−0.9338	−0.9476		
1.30	−0.8596	−0.8953	−0.9143			

at $T \simeq 0.89$, which agrees with previously computed[4,10] values for T_c. It is helpful to examine the data in the following slightly different way. We use

$$\mathcal{S} = cL^{2-\eta}, \tag{2.8}$$

valid for $T < T_c$, and plot $[\ln(\mathcal{S}) - \ln(c)]/\ln L$ versus T, to obtain $2-\eta$. All the data points fall, within statistical errors, into a universal curve (see Fig. 3) at low temperatures for

$$\ln(c) \simeq -0.20 . \tag{2.9}$$

Figure 3 has two virtues: (i) one can see the values of the statistical errors in η and (ii) it shows clearly that for $T \gtrsim 0.9$, Eq. (2.8) fails, as it must for $T > T_c$, whence one gets an independent estimate of the value of T_c, and of $\eta(T_c)$.

We read from Fig. 3,

$$T_c = 0.89 \pm 0.02 \tag{2.10}$$

and

$$\eta(T_c) \simeq 0.24 \pm 0.3 . \tag{2.11}$$

We shall return to these numbers in Sec. III. We shall arrive there at the value quoted here for T_c via an independent route.

C. Value of ν

We next describe three different procedures we have followed to arrive at a value of ν. To obtain ν, one might try plotting $\ln(\mathcal{S})$ versus $(T-T_c)^{-\nu}$ for various values of T_c and ν. Note that for $\xi \ll L$, $\ln(\mathcal{S}) \sim \ln(\xi)$, whence, using Eq. (1.3), it follows that $\ln(\mathcal{S}) \sim (T-T_c)^{-\nu}$. Unfortunately, fulfillment of $\xi \ll L$ requires that the most relevant data, that in the neighborhood of T_c, be neglected, unless one deals with macroscopic systems. Good experimental data fits have been obtained in the past using such procedures with experimentally determined values of T_c and $\nu = 0.5$. Figure 4 shows such a plot, using our data of Table I, for $T_c = 0.89$ and $\nu = 0.5$. Size effects are obvious. Our results seem to be size independent for $L = 200$ and $(T-T_c)^{-\nu} \lesssim 3$, which corresponds to $(T/T_c) \gtrsim 1.1$. The other end point of the data corresponds to $(T/T_c) \simeq 1.4$. This is a small temperature range [$(T-T_c)^{-\nu}$ only changes by a factor of 2 here, but note that it does not change by more than a factor of 3 or 4 in data analysis of experimental work], and furthermore it only comes within 10% of T_c.

The data points in Fig. 4, which do not suffer from finite-size effects, all fall into the same straight line, as they should. The same data points all fall into one straight line if T_c and ν are changed as long as the following equation is satisfied:

$$T_c = 0.89 + 0.1(0.5 - \nu) . \tag{2.12}$$

Since the error in T_c is 0.02, we allow ν to vary only by ± 0.2. In addition, variations in the value of ν smaller than about 0.2, keeping T_c fixed, do not seriously affect the fits. This method yields $\nu = 0.5 \pm 0.3$. The error, which is unfortunately large, accounts for both incoherent

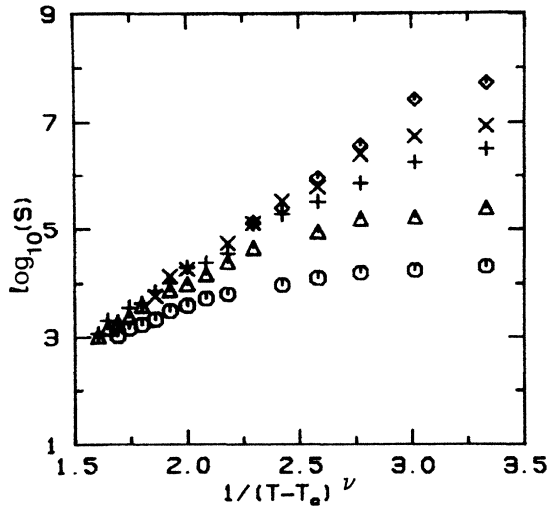

FIG. 4. Quantity $\ln(\mathcal{S})$ versus $(T-T_c)^{-\nu}$ is shown for $\nu=0.5$ and $T_c=0.89$ for systems of $L=200$ (◇), $L=90$ (×), $L=60$ (+), $L=30$ (△), and $L=15$ (○). Size dependence is obvious in these data points.

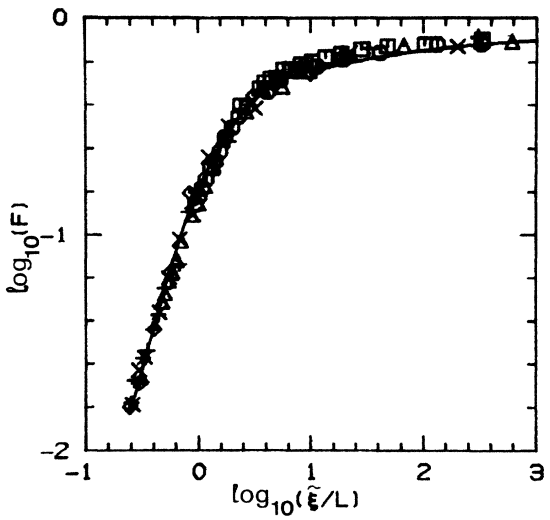

FIG. 5. Logarithm (base 10) of the scaling function F, defined in Eq. (1.4) is plotted versus $\log_{10}(\tilde{\xi}/L)$ for $\nu=0.5$, $T_c=0.89$, and $b=1.7$, for systems of $L=6$ (□), $L=15$ (○), $L=30$ (△), $L=60$ (+), $L=90$ (×), and $L=200$ (◇). The solid line is a cubic spline fit to the $L=200$ data.

sources.

The main weakness of the above procedure is that it does not allow us to use the data produced by our MC simulations in the most relevant region: the close neighborhood of T_c. We now turn to finite-size scaling.[11]

In the procedure that follows, we assume the functional dependence $\xi(T)$, Eq. (1.3), predicted by KT, and a set of values for b, T_c and ν. Now, it follows from Eq. (1.4) that $\mathcal{S}/L^{2-\eta}$ is a universal function of $\tilde{\xi}/L$. If a set of values for b, T and ν, does not yield a universal function $F(\tilde{\xi}/L)$ for $S/L^{2-\eta}$, those values are ruled out. The critical value $\eta_c=\frac{1}{4}$ is used. Figure 5 exhibits $\log_{10}(F)$ versus $\log_{10}(\tilde{\xi}/L)$ for $T_c=0.89$, $b=1.70$, and $\nu=0.5$. Indeed, F seems to be a good universal function, within statistical errors, of $\tilde{\xi}/L$. Note that $\tilde{\xi}/L$ covers the range 10^{-1} to 10^3. Similarly good fits can be obtained if ν and T_c fulfill Eq. (2.12).

For instance, Fig. 6 exhibits the results obtained for $\nu=0.2$ and $T_c=0.92$ if we set $b=5.7$, and Fig. 7 corresponds to $\nu=0.9$, $T_c=0.85$ and $b=0.7$. Thus, our error in T_c (0.02) again, produces an error of about 0.2 in ν. In addition, given a value of T_c, we have found that variations of ν within 0.1 of its best value are acceptable. These two incoherent sources of error in ν lead to $\Delta\nu\approx 0.2$. We are therefore led by this method to the value $\nu=0.5\pm 0.2$.

The results shown in Fig. 8 follow from assuming the non-KT form

$$\tilde{\xi}=(T-T_c)^{-\nu} \tag{2.13}$$

for $T_c=0.93$ and $\nu=1.6$. Looking up this value of T_c in Fig. 2 yields $\eta_c=0.29$. The value of the critical exponent $\gamma=2.7$ for the divergence of $\mathcal{S}$, follows from the scaling relation $\gamma=\nu(2-\eta)$ for $d=2$. This value of γ is rather close to the values obtained by Rogiers *et al.*,[19] but much bigger than the value $\gamma=1.4$ computed by Tobochnick and Chester.[4] The fact that the method just described cannot discriminate between the KT prediction for $\xi(T)$ and the algebraic form shown in Eq. (2.13) is a shortcoming of this method.

The weakness of the above procedure is that it has too many parameters (b and T_c) in addition to ν, and we do not know T_c very accurately. We next use a procedure based on finite-size scaling which does not depend on the value of T_c; indeed, ν is the only fitting parameter.

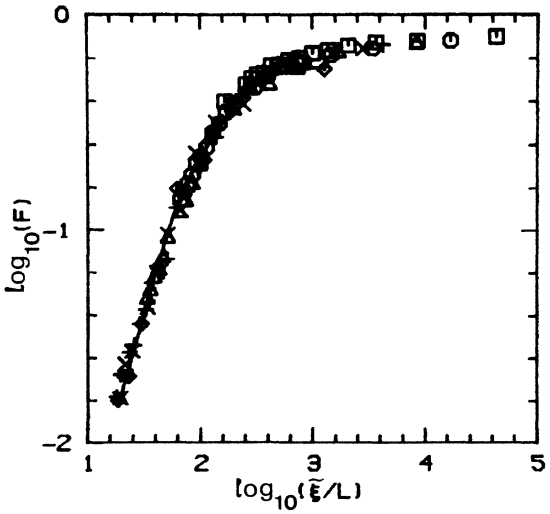

FIG. 6. Logarithm (base 10) of the scaling function F, defined in Eq. (1.4) is plotted versus $\log_{10}(\tilde{\xi}/L)$ for $\nu=0.2$, $T_c=0.92$, and $b=5.7$, for systems of $L=6$ (□), $L=15$ (○), $L=30$ (△), $L=60$ (+), $L=90$ (×), and $L=200$ (◇). The solid line is a cubic spline fit to the $L=200$ data.

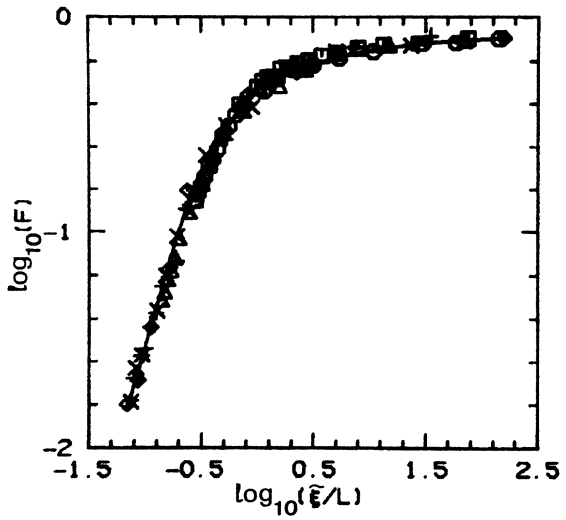

FIG. 7. Logarithm (base 10) of the scaling function F, defined in Eq. (1.4) is plotted versus $\log_{10}(\tilde{\xi}/L)$ for $\nu=0.9$, $T_c=0.85$, and $b=0.70$. ⊡ is for $L=6$, ⊙ is for $L=15$, △ is for $L=30$, + is for $L=60$, × is for $L=90$, and ◇ is for $L=200$. The solid line is a cubic spline fit to the $L=200$ data points.

Consider the quantity[20]

$$\Lambda=-\frac{\partial \ln(\mathscr{S})}{\partial T} . \tag{2.14}$$

Substitution of Eq. (1.4) yields

$$\Lambda=\frac{d\eta}{dT}\ln(L)-\frac{\partial \ln(F)}{\partial \ln(\tilde{\xi}/L)}\frac{\partial \ln(\tilde{\xi}/L)}{\partial T} . \tag{2.15}$$

Since good universal functions were obtained above using $\eta(T)=\eta_c$ for $T\geq T_c$, we neglect the first term above. Then,

$$\Lambda\simeq-\frac{\partial \ln(F)}{\partial \ln(\tilde{\xi}/L)}\frac{\partial \ln(\tilde{\xi}/L)}{\partial T} . \tag{2.16}$$

Consider now the non-KT form for $\tilde{\xi}(T)$ of Eq. (2.13), then

$$\Lambda\sim\frac{\nu}{T-T_c}\left[\frac{\partial \ln(F)}{\partial \ln(\tilde{\xi}/L)}\right] , \tag{2.17}$$

which using Eq. (2.13) again, can be written as follows:

$$\Lambda=L^{1/\nu}F_2(\tilde{\xi}/L) , \tag{2.18}$$

where F_2 is some function. If follows then that the maximum value of Λ versus T corresponds to $\tilde{\xi}/L=$const, the maximum value (Λ_m) of $\Lambda(T)$ for each value of L must fulfill

$$\ln(\Lambda_{\max})\sim\frac{1}{\nu}\ln(L) . \tag{2.19}$$

Figure 9 exhibits Λ versus T for $L=6$, 15, 30, 60, 90, and 200. Figure 10 exhibits $\ln(\Lambda_{\max})$ versus $\ln(L)$. The points shown do not fall on a straight line as they should if Eq. (2.19) were fulfilled.

On the other hand, consider the form of $\tilde{\xi}(T)$ predicted by KT, then, Eq. (2.14) becomes,

$$\Lambda\sim\frac{\partial \ln(F)}{\partial \ln(\tilde{\xi}/L)}\frac{\nu b}{(T-T_c)^{\nu+1}} . \tag{2.20}$$

Substitution of (1.3) for $\tilde{\xi}(T)$ yields

$$\Lambda\sim F_3(\tilde{\xi}/L)[\ln(\tilde{\xi})]^{(1+1/\nu)} , \tag{2.21}$$

where

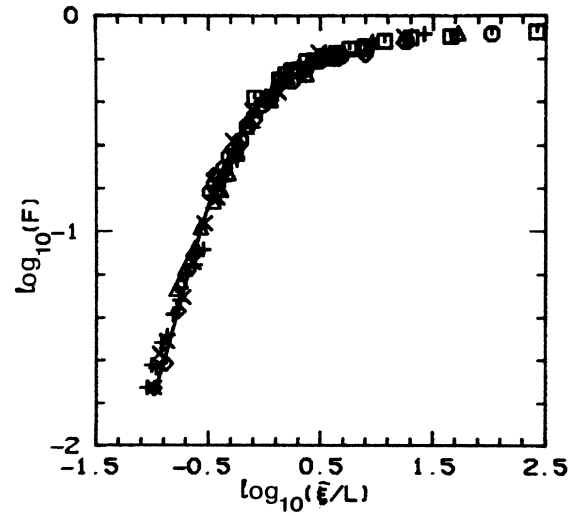

FIG. 8. Data points that follow from assuming the algebraic temperature dependence of $\tilde{\xi}(T)$ expressed in Eq. (2.13); ⊡ is for $L=6$, ⊙ is for $L=15$, △ is for $L=30$, + is for $L=60$, × is for $L=90$, and ◇ is for $L=200$. The solid line is a cubic spline fit to the $L=200$ data points.

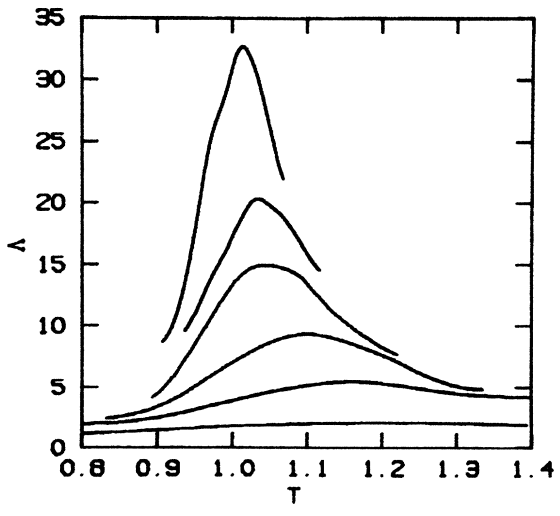

FIG. 9. Derivatives of cubic spline fits to $\ln(\mathscr{S})$ versus T yield the curves shown for $\Lambda=-\partial \ln\mathscr{S}/\partial T$ for systems of $L=6$, 15, 30, 60, 90, and 200. The most sharply peaked curve corresponds to $L=200$, the second highest peaked to $L=90$, and so on to the lowest curve which is almost flat and corresponds to $L=6$.

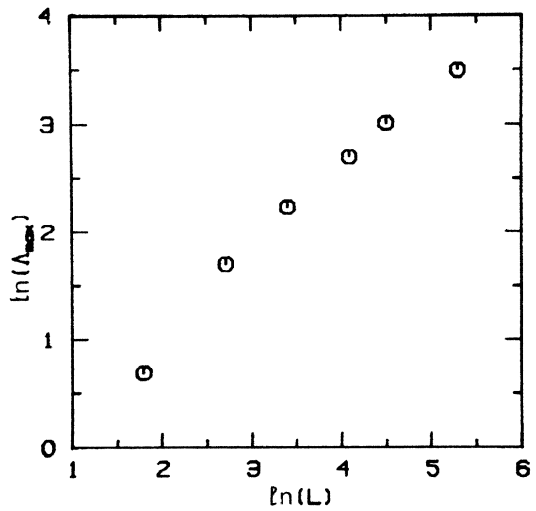

FIG. 10. Logarithm of the maxima of Λ versus T shown in Fig. 9 are exhibited here versus $\ln(L)$ to test the validity of Eq. (2.18) which is based on Eq. (2.13). Failure of the data points shown to fall on a straight line is our basis for rejecting the validity of Eq. (2.13).

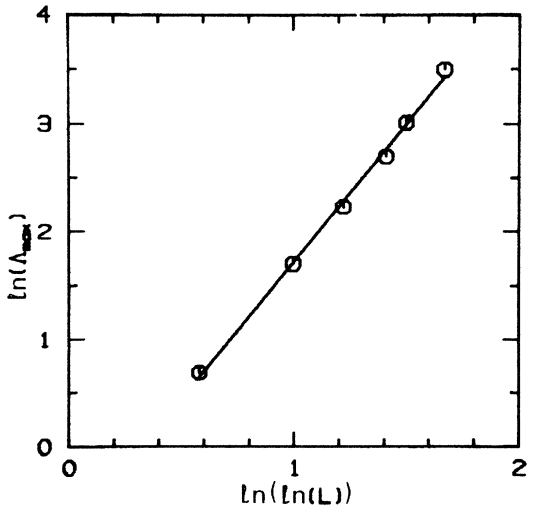

FIG. 11. Logarithm of the maxima of Λ vs T (taken from Fig. 9) are exhibited here versus $\ln\ln(L)$. A straight line is shown as a guide to the eye. The errors in the data points are given by the size of the circles shown.

$$F_3(\tilde{\xi}/L)=\frac{\partial \ln(F)}{\partial \ln(\tilde{\xi}/L)} . \tag{2.22}$$

Adding and subtracting $\ln(L)$ within the square brackets leads to the desired expression

$$\Lambda \sim F_3(\tilde{\xi}/L)[\ln(\tilde{\xi}/L)+\ln(L)]^{(1+1/\nu)} . \tag{2.23}$$

Let $(\tilde{\xi}/L)_m$ be defined by $\Lambda[(\tilde{\xi}/L)_m] > \Lambda(\tilde{\xi}/L)$. Equation (2.23) implies that $(\tilde{\xi}/L)_m$ decreases toward its asymptotic value as L increases, in qualitative agreement with Szeto and Dresselhaus.[12] To obtain $(\tilde{\xi}/L)_m$, we use the results shown in Fig. 9, Eq. (1.3), $b=1.7$, $\nu=0.5$, and $T_c=0.89$. The results obtained are summarized reasonably well by the relation $(\tilde{\xi}/L)_m \simeq 1+10L^{-1}$. We can therefore neglect $\ln(\tilde{\xi}/L)$ in Eq. (2.23) for $L \ln L \gg 10$. It follows that

$$\ln(\Lambda_{\max}) \sim \left[1+\frac{1}{\nu}\right] \ln|\ln(L)| \tag{2.24}$$

for L large.

Figure 11 shows $\ln(\Lambda_{\max})$ versus $\ln[\ln(L)]$. The data points fall near a straight line, even for small L, where some deviations are expected. Lest it be thought that the near-straight-line behavior is a consequence of having taken too many (two) logarithms of L for the abscissa in Fig. 11 it is worth remarking that a plot of $\ln(\Lambda_{\max})$ versus $\ln\ln\ln L$ shows data points on a markedly *curved* line.

To arrive at a value of ν, let ν_L be the value of ν we obtain from the slope $(1+1/\nu)$ of the best straight-line fit to the data shown in Fig. 11 excluding the points corresponding to lengths smaller than L. Figure 12 exhibits ν_L versus $1/L$. The $(1/L)\to 0$ limit of ν_L is the desired value of ν. From Fig. 12, we read off,

$$\nu=0.5\pm 0.1 . \tag{2.25}$$

Note that the error bars for ν_L in Fig. 12 increase in size as L increases. This is so because the number data points decrease as L increases, leading to increasing statistical errors in the slope $(1+1/\nu)$ of the best fit.

Finally, we summarize how to use the numbers we obtained to predict experimental results on finite systems. First note that the magnetic susceptibility (χ) is related to $\mathcal{S}$ by $2T\chi=\mathcal{S}$. For $T \le T_c$, $\mathcal{S}$ is given by Eqs. (2.8) and (2.9), and $\eta(T)$ can be extracted from Figs. 2 or 3. For $T > T_c$, Eq. (1.4), $\eta=\frac{1}{4}$, in addition to the values of $F(x)$ and other relevant parameters given in Table III

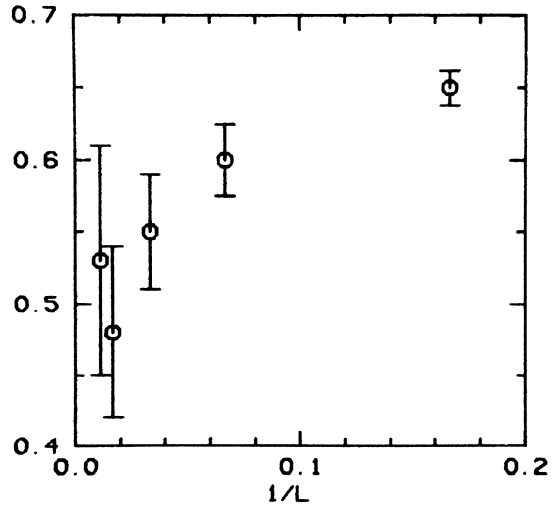

FIG. 12. Sloped straight-line fits to the data shown in Fig. 11 yield values of $1+1/\nu$. We show here ν_L (the value obtained for ν if all data points corresponding to systems of length smaller than L are excluded from the fit) versus L. For instance, the point shown for $1/L=\frac{1}{90}$ corresponds to a fit including only the points for $L=90$ and $L=200$ in Fig. 11.

TABLE III. Values of the logarithm (base 10) of the scaling function $F(x)$. The definition of F, its asymptotic behavior, as well as values of parameters necessary to compute the correlation length ξ and $\mathscr{S}$, defined in Eq. (1.1), for any finite system, are included for convenience. For $T \leq T_c$, $\mathscr{S} = cL^{2-\eta}$, $c=0.82$, η is given in Fig. 2. For $T \geq T_c$, $\mathscr{S} = L^{2-\eta_c} F(\tilde{\xi}/L)$, $\eta_c = 0.25$, $\tilde{\xi} = \exp[b/(T-T_c)^{\nu}]$, $b=1.70$, $T_c = 0.89$, $\nu = 0.5$, $F(x) \to 0.72x^{2-\eta_c}$ for $x \lesssim 0.2$, $F(\infty) = 0.82$.

$\log_{10}(x)$	$\log_{10}F(x)$	$\log_{10}(x)$	$\log_{10}F(x)$
−0.6	−1.76	0.7	−0.28
−0.5	−1.60	0.8	−0.25
−0.4	−1.43	0.9	−0.23
−0.3	−1.27	1.0	−0.21
−0.2	−1.11	1.1	−0.19
−0.1	−0.97	1.2	−0.18
0.0	−0.83	1.3	−0.16
0.1	−0.71	1.4	−0.15
0.2	−0.60	1.5	−0.14
0.3	−0.51	1.6	−0.14
0.4	−0.43	1.7	−0.13
0.5	−0.37	1.8	−0.13
0.6	−0.32	1.9	−0.12
		2.0	−0.12

yield $\mathscr{S}$ in the neighborhood of T_c for any value of L. The numbers shown for $F(x)$ in Table III follow from the best cubic spline fit to all the data points in Fig. 5.

III. CONCLUSIONS

Our main result is the value of the critical index, $\nu = 0.5$. We have been able to reduce the error in ν to 0.1 using a procedure, described in Sec. II, based on finite-size scaling. This procedure does not rely on the value of T_c. Thus, we can now return to the second procedure used in Sec. II, and which using the determined value of ν can now be turned around to determine T_c. Then, we get $T_c = 0.89$, and since $\Delta\nu = 0.1$, the error in T_c turns out—see Eq. (2.12) and below—to be 0.02. This independently determined value of T_c can in turn be used to obtain, from the data shown in Fig. 2, the value of $\eta(T_c)$ quoted in Eq. (2.11).

The procedure we have followed in Sec. III, examining the behavior of $\Lambda_{\max}$ as a function of L to determine ν, should prove useful analyzing data from experiments on systems, such as Josephson-junction arrays, which are not extremely large. Thus, rather than performing experiments only on arrays of $L = 10^3$, say, it will prove useful to do experiments on several systems of different sizes, much as we have done here.

All simulation for systems of 200×200 spins were carried out at IBM Yorktown Heights. All other simulations were performed on a VAX-380.

ACKNOWLEDGMENTS

We are indebted to Dr. S. Solla and Dr. J. José for many helpful comments. We are also grateful to Dr. R. J. Creswick and Dr. R. Angulo for reading the manuscript. Dr. R. Medina has helped us with our data analysis by letting us use some of his computer programs. We acknowledge having used a VAX-380 granted to our Institute [Instituto Venezolano Investigaciones Científicas (Caracas, Venezuela (IVIC)] by the Consejo Nacional de Investigaciones Científicas y Tecnológicas. One of us (J.S.) wishes to thank the IBM Thomas J. Watson Research Center for their hospitality.

*Also at Universidad Simón Bolívar, Sartenejas, Caracas 1080A, Venezuela.

†Present address: Departamento de Fisica, Universidade de Porto, Porto, Portugal.

‡On sabatical leave from Centro de Física, Instituto Venezolano de Investigaciones Científicas, Apartado 1827, Caracas 1010A, Venezuela.

[1]J. M. Kosterlitz and D. J. Thouless, J. Phys. C **6**, 1181 (1973); J. M. Kosterlitz, *ibid.* **7**, 1046 (1974); for the relation between these two papers, see, A. P. Young, Phys. Rev. B **19**, 1885 (1979).

[2]J. José, L. P. Kadanoff, S. Kirkpatrick, and D. R. Nelson, Phys. Rev. B **16**, 1217 (1977); J. Villain, J. Phys. (Paris) **36**, 581 (1975); S. A. Solla and E. K. Riedel, Phys. Rev. B **23**, 6008 (1981); see also, P. Minnhagen, *ibid.* **32**, 3088 (1985).

[3]For a review, see M. N. Barber, Phys. Rep. (Netherlands) **59**, 376 (1980).

[4]J. Tobochnik and G. V. Chester, Phys. Rev. B **20**, 3761 (1979).

[5]For instance, W. J. Camp and J. P. Van Dyke, J. Phys. C **8**, 336 (1975); C. J. Hamer and J. Kogut, Phys. Rev. B **20**, 3859 (1979).

[6]D. J. Bishop and J. D. Reppy, Phys. Rev. Lett. **40**, 1727 (1978). See G. Agnolet, D. C. McQueency, and J. D. Reppy, Phys. Rev. Lett. **52**, 1325 (1984); D. Finotello and F. M. Gasparini, *ibid.* **55**, 2156 (1985).

[7]A. F. Hebard and A. T. Fiory, Phys. Rev. Lett. **50**, 1603 (1983); A. T. Fiory, A. F. Hebard, and W. I. Glaberson, Phys. Rev. B **28**, 5075 (1983).

[8]R. F. Voss and R. A. Webb, Phys. Rev. B **25**, 3446 (1982); D. W. Abraham, C. J. Lobb, M. Tinkham, and T. M. Klapwijk, *ibid.* **26**, 5268 (1982); R. A. Webb, R. F. Voss, G. Grinstein, and P. M. Horn Phys. Rev. Lett. **51**, 690 (1983); C. J. Lobb, Physica **126B**, 319 (1984).

[9]D. R. Nelson and J. M. Kosterlitz, Phys. Rev. Lett. **39**, 120 (1977); B. I. Halperin and D. R. Nelson, J. Low Temp. Phys. **36**, 1165 (1979); C. J. Lobb, D. W. Abraham, and M. Tinkham, Phys. Rev. B **27**, 150 (1983); V. Ambegaokar, B. I. Halperin, D. R. Nelson, and E. D. Siggia, *ibid.* **21**, 1806 (1980); T. Ohta and D. Jasnow, *ibid.* **20**, 139 (1979).

[10]W. J. Shugard, J. D. Weeks, and G. H. Gilmer, Phys. Rev., Lett. **48**, 1399 (1978); however, a value of T_c about 10% higher was obtained by Van Himbergen, J. Phys. C **17**, 5039 (1984).

[11]M. P. Nightingale and H. W. J. Blote, Physica **104A**, 352 (1980); V. Privman and M. E. Fisher, Phys. Rev. B **30**, 322 (1984).

[12]K. Y. Szeto and G. Dresselhaus Phys. Rev. B **32**, 3142 (1985).

[13]This is a finite-size effect; it clearly does not prevent the vortex density from vanishing, as it must, in the $L \to \infty$ limit. For a discussion of this point, see D. W. Abraham, Division of Applied Sciences, Harvard University, Technical Report Number 23 (unpublished).

[14]N. Metropolis, A. W. Rosenbluth, M. N. Rosenbluth, A. H. Teller, and E. Teller, J. Chem. Phys. **21**, 1087 (1953).

[15]Concern over whether running times in Monte Carlo simulations are sufficiently long compared to the time it takes slow moving vortices to drift over the length of the system has been expressed in, C. Kawabata and K. Binder, Solid State Commun. **22**, 705 (1977); D. R. Nelson, Phys. Rev. B **26**, 269 (1982). Following Nelson's suggestion, a MC simulation was performed: K. J. Strandburg, S. A. Solla, and G. V. Chester, Phys. Rev. B **28**, 2717 (1983).

[16]This definition of τ is reasonable for relaxation processes which are not necessarily exponential, as has been suggested by S. Kirkpartrick, in *Ordering in Strongly Fluctuating Condensed Matter Systems,* edited by T. Riste (Plenum, New York, 1980).

[17]Part of the argument given here follows from Nelson's paper (Ref. 15).

[18]This value is of the same order of magnitude as the value suggested for the "glide" diffusivity of dislocations, in R. Bruinsma, B. I. Halperin, and A. Zippelius, Phys. Rev. B **25**, 579 (1982), if one Monte Carlo step per spin is equated with 10^{-10} sec.

[19]J. Rogiers, E. W. Grundke, and D. D. Betts, Can. J. Phys. **57**, 1719 (1979).

[20]Quantity Λ was originally used in J. F. Fernández, Phys. Rev. B **25**, 417 (1982).